



Empirical Analysis of Client-based Network Quality Prediction in Vehicular Multi-MNO Networks

Benjamin Sliwa and Christian Wietfeld

Communication Networks Institute, TU Dortmund University, 44227 Dortmund, Germany

e-mail: {Benjamin.Sliwa, Christian.Wietfeld}@tu-dortmund.de

Abstract—Multi-Mobile Network Operator (MNO) networking is a promising method to exploit the joint force of multiple available cellular data connections within vehicular networks. By applying anticipatory communication principles, data transmissions can dynamically utilize the mobile network with the highest estimated network performance in order to achieve improvements in data rate, resource efficiency, and reliability.

In this paper, we present the results of a comprehensive real-world measurement campaign in public cellular networks in different scenarios and analyze the performance of online data rate prediction based on multiple machine learning models and data aggregation strategies. It is shown that multi-MNO approaches are able to achieve significant benefits for all considered network quality and end-to-end indicators even in the presence of a single dominant MNO. However, the analysis points out that anticipatory multi-MNO communication requires the consideration of MNO-specific machine learning models since the impact of the different features is highly depending on the configuration of the network infrastructure.

I. INTRODUCTION

Anticipatory communication [1] has been proposed as a method to face the various challenges of next-generation networks, which are related to higher requirements (e.g., latency and data rate as enablers for autonomous driving) as well as massive increases in the overall data usage [2]. This novel communication paradigm aims to optimize decision processes within communication networks by proactively integrating context information such as mobility predictions and network quality parameters. Applications range from opportunistic sensor data transfer for optimizing the coexistence of different cell users [3] to reliable and mobility-aware multi-hop routing [4]. Since anticipatory communications is a *data-driven* approach, it relies on knowledge and prediction models. In recent work [5], [6], we have demonstrated the potentials of using machine learning-based data rate prediction and multi-layer connectivity maps for improving the resource-efficiency of vehicular sensor data transmissions. Furthermore, we have shown that the prediction models can be exploited for analyzing novel communication methods in close to reality scenarios [7]. In this paper, we provide an empirical analysis of the potentials of using data rate prediction within multi-connectivity cellular vehicular networks. The real world evaluation is carried out in the public cellular networks of the three MNOs in Germany and paves the way for future development of context-aware multi-connectivity optimizations. It furthermore shows how upcoming 5G-based vehicular communication systems can exploit multi-connectivity for compensating coverage gaps.

Fig. 1 shows an example trace of the Long Term Evolution (LTE) Reference Signal Received Power (RSRP) for three different MNOs during a drive test in a suburban environment. It can be seen that although not all carriers are able to

guarantee seamless connectivity for the whole experiment duration, a multi-carrier approach is able to do so. The contributions provided by this paper are as follows:

- Comprehensive **real world performance evaluation of vehicular multi-MNO communication** in the public cellular LTE networks of German MNOs.
- Statistical analysis of the potential benefits by combining networks of multiple MNOs and data management techniques using multi-MNO Connectivity Maps (CMs)
- Performance evaluation of **client-based online data rate prediction** with different data aggregation methods and machine learning models.
- For achieving a high grade of transparency and reproducibility, all raw results of the measurements and the measurement application itself are provided in an **Open Access** way.

The remainder of the paper is structured as follows. After discussing relevant approaches for machine learning-based data rate prediction and evaluations of multi-connectivity approaches in Sec. II, we present the methodological model for the empirical performance evaluation in Sec. III. The result analysis is divided into two parts. At first, the statistical properties of the network quality indicators, potential benefits of using multi-MNO connectivity as well as methods for maintaining multi-MNO data are discussed in Sec. IV. Afterwards, machine learning-based data rate prediction is discussed in Sec. V. The analysis includes the application of different prediction models in uplink and downlink direction as well as data aggregation and feature importance evaluations.

II. RELATED WORK

Since anticipatory communication highly relies on predicting unobserved values from measurable information, it is

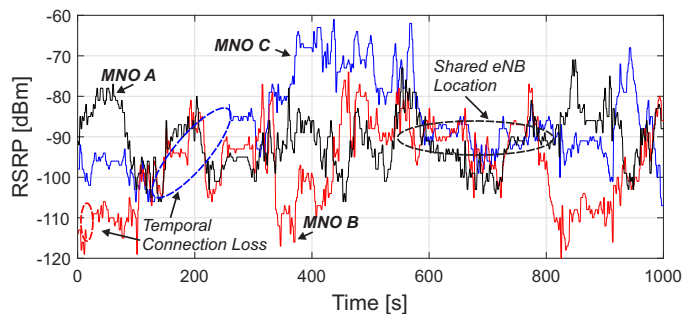


Fig. 1. Example RSRP trace for three different network carriers in suburban environment. Although individual networks fail to provide connectivity at certain locations, the combined approach is able to provide full coverage.

closely related to machine learning [8]. A comprehensive overview about different machine learning models and their application fields in wireless communication networks is provided by [9].

Within vehicular networks, the performance of end-to-end indicators such as throughput and latency is highly impacted by the encountered network quality [10], [11]. Therefore, many research works investigate passive data rate prediction based on measured network quality indicators, e.g. for interface selection [12]. A survey about different bandwidth estimation techniques is provided by [13].

The authors of [14] evaluate different machine learning models (Artificial Neural Networks (ANNs), Linear Regression (LR) and Random Forests (RF)) for predicting the downlink data rate on a large data set using signal quality measurements only. They conclude that classical machine learning methods yield excellent prediction results – with the RF model achieving the lowest error probability – for providing the MNO with additional information. However since no information about the payload size about the transmitted packets is provided, it can be assumed that a fixed size was used for the experiments. As other work has shown [3], [5], [6] the payload size is an important feature that needs to be considered in order to derive models, which generalize well on other data sets. A simple linear regression approach based on OpenSignal data is proposed in [15]. While the authors point out that the RSRP seems to have the dominant effect on prediction accuracy, they argue that a better compensation of multipath-effects could be achieved by integrating additional indicators (e.g., Reference Signal Received Quality (RSRQ), Signal-to-interference-plus-noise Ratio (SINR)) into the prediction. The authors of [16] present a real world measurement campaign for cellular bandwidth estimation in vehicular environments for two different MNOs. While the achieved prediction accuracy is relatively low due to the focus on solely radio-related features, it is shown that the observed behavior differs depending on the MNO. Similar to the work discussed in [17], the RF model achieves the best prediction accuracy. This fact is confirmed by [18] Kousias et al., who point out that the relevance of the individual features is highly depending on the MNO. Fur-

thermore, daytime-specific aspects are evaluated. In [19], the authors analyze passive LTE data rate prediction as a metric for interface selection within highly mobile networks. While the considered ANN approach achieves the highest accuracy, the authors present a LR-based approach as a lightweight alternative for online application. However, the size of the training set is low and the authors do not consider the packet size within their prediction mechanism.

Although vehicles are able to measure the current channel context and can apply methods to estimate their trajectories, they are not able to directly measure the network quality at future locations. Connectivity maps [20] provide a way to map location data to network quality information. They are often created using a crowdsensing approach and are utilized as a priori information [21], allowing to make network quality forecasts based on previous measurement in the same geospatial area [5].

III. METHODOLOGY OF THE EMPIRICAL EVALUATION

In this section, the methodological aspects of the measurement campaign are explained. For the empirical performance evaluation, drive tests are performed in four scenarios with different velocity profiles and building densities: *campus* (3 km), *urban* (3 km), *suburban* (9 km), *highway* (14 km), whereas each track is evaluated ten times.

During the drive tests, three Android-based User Equipments (UEs) (Samsung Galaxy S5 Neo, Model SM-G903F), which use the cellular link of one of the considered MNOs, are used to capture the network quality indicators and perform the transmissions for data rate and Round Trip Time (RTT) evaluations. Each 10 s, the measurement application¹ performs Transmission Control Protocol (TCP) transmissions in uplink and downlink direction with variable payload sizes in the range of 0.1 MB to 10 MB. The data transfer is performed in the public cellular network and the throughput is calculated on the server side. RTT is measured on the transport layer. Transmissions are only performed if a valid LTE connection is present. In total, 12938 transmissions (58.45 GB) are

¹Measurement software available at <https://github.com/BenSliwa/MTCApp>

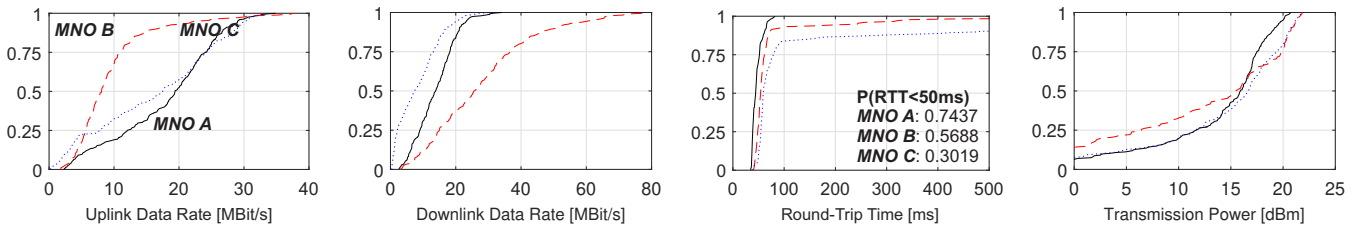


Fig. 2. Urban scenario: Empirical Cumulative Distribution Functions (ECDFs) of different indicators for the considered MNOs.

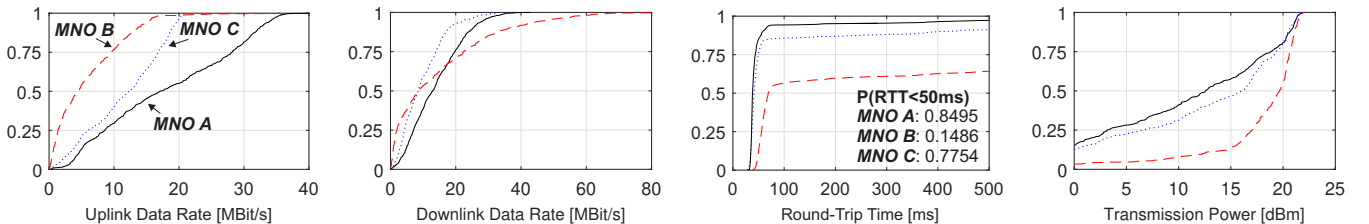


Fig. 3. Highway scenario: ECDFs of different indicators for the considered MNOs.

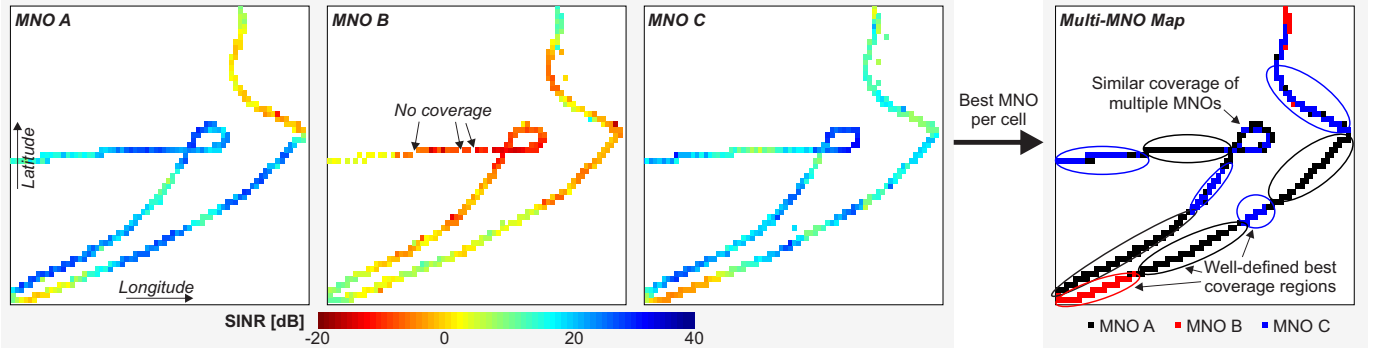


Fig. 4. Excerpt of the connectivity maps of the highway track for all considered MNOs. The average SINR per cell is shown as an example network quality indicator. The operator map visualizes the MNO with the highest SINR per cell.

performed on a total driven distance of 287 km. The raw real world measurements, which consist of time series data for trajectories and network quality indicators, can be accessed via [22].

For performing the machine learning-related evaluation, Waikato Environment for Knowledge Analysis (WEKA) [23] and LIBSVM [24] are used.

IV. STATISTICAL ANALYSIS OF MULTI-MNO VEHICULAR NETWORKING

In this section, the results and network quality characteristics are analyzed from a statistical perspective. In addition, potential benefits of using multi-MNO communication in vehicular networks are discussed.

A. Statistical Properties

Due to spacial constraints, we focus on comparing two example scenarios *campus* (see Fig. 2) and *highway* (see Fig. 3). The figures show the ECDFs for data rates in uplink and downlink direction, RTT and applied transmission power P_{TX} . While *MNO A* provides a similar network performance in both scenarios, the results for *MNO B* and *MNO C* are highly scenario-dependent and directly related to the LTE coverage (cf. Tab. I). In the highway scenario, the overall LTE coverage of *MNO C* is only 92 %. Therefore, multiple handovers to 3G occurred during active transmissions, which is the reason for the high RTT and the low throughput of *MNO B*. Note that RTT is measured on the transport layer and is therefore impacted by the network quality and TCP-related features such as retransmissions. Due to the low coverage, the average distance to the serving evolved Node B (eNB) is high. Therefore, the UE aims to compensate the path loss by increasing the transmission power P_{TX} , which is much higher for *MNO B* than for the other considered MNOs. As discussed in [25], P_{TX} has a dominant impact on the overall power consumption of the UE. In the highway scenario, it can be expected that using *MNO B* leads to a significantly shorter battery lifetime, which also fits our qualitative observations during the measurements.

B. Multilayer Multi-MNO Connectivity Maps

The acquired data is utilized to create a multilayer multi-MNO connectivity map. Each layer contains the measurements of one specific Key Performance Indicator (KPI), which are aggregated geospatially based on a defined cell size c . Fig. 4 shows an excerpt of the SINR layer of the CMs for the

different MNOs. The cell-wise determination of the best MNO finally leads to the multi-MNO map.

A straightforward estimation of achievable benefits by using the derived multi-MNO CM for context-aware network selection is provided by Tab. I, which shows the behavior of the network quality metrics RSRP, RSRQ, SINR and Channel Quality Indicator (CQI) as well as of multiple end-to-end indicators. For each vehicle position within the real world traces, the statistical approach selects the MNO with the best network performance for the considered indicator.

TABLE I
NETWORK QUALITY INDICATORS AND ACTIVE MEASUREMENTS FOR DIFFERENT INDIVIDUAL AND COMBINED MNOs.

Indicator	MNO A		MNO B		MNO C		Multi MNO
	Mean	Best	Mean	Best	Mean	Best	
Coverage	1.0	-	0.96	-	0.91	-	1.0
RSRP [dBm]	-87.6	0.525	-97.1	0.19	-91.4	0.285	-82.6
RSRQ [dB]	-7.5	0.684	-9.85	0.2	-10.7	0.116	-6.69
SINR [dB]	14	0.556	7.23	0.229	7.43	0.216	18.2
CQI	10.1	0.491	9.25	0.317	8.32	0.191	12.2
RTT [ms]	57.4	0.652	380	0.159	459	0.189	43.6
P_{TX} [dBm]	12.4	0.434	16.5	0.201	13.8	0.365	8.91

Best: Proportion of the MNO providing the best metric value of all MNOs.

Although the mean RTT of *MNO B* and *MNO C* is much higher than the one of *MNO A*, the multi-MNO is still able to improve the average behavior of all considered indicators. In addition, the mean RTT is reduced by 24 % and the average transmission power P_{TX} is reduced by 28 %.

V. CLIENT-BASED ONLINE DATA RATE PREDICTION

In this section, the results and insights of Sec. IV are exploited for predicting the end-to-end data rate. Furthermore, the importance of the individual features is analyzed and multi-MNO CMs are exploited to optimize the prediction accuracy.

Machine learning-based throughput prediction is a regression task. In the following, we analyze the performance of the ANN [26], M5 Regression Tree (M5) [27], RF [28], and Support Vector Machine (SVM) [29] models. The prediction process is shown in Fig.6. During the *training* phase, active data transmissions are performed and the resulting throughput and RTT are captured and used as the *labels* for the prediction. The actual training of the learning models is performed offline. The trained models are applied online during the *application* phase. The parameters of all considered models are optimized in a preprocessing step. For the ANN, a deep neural network

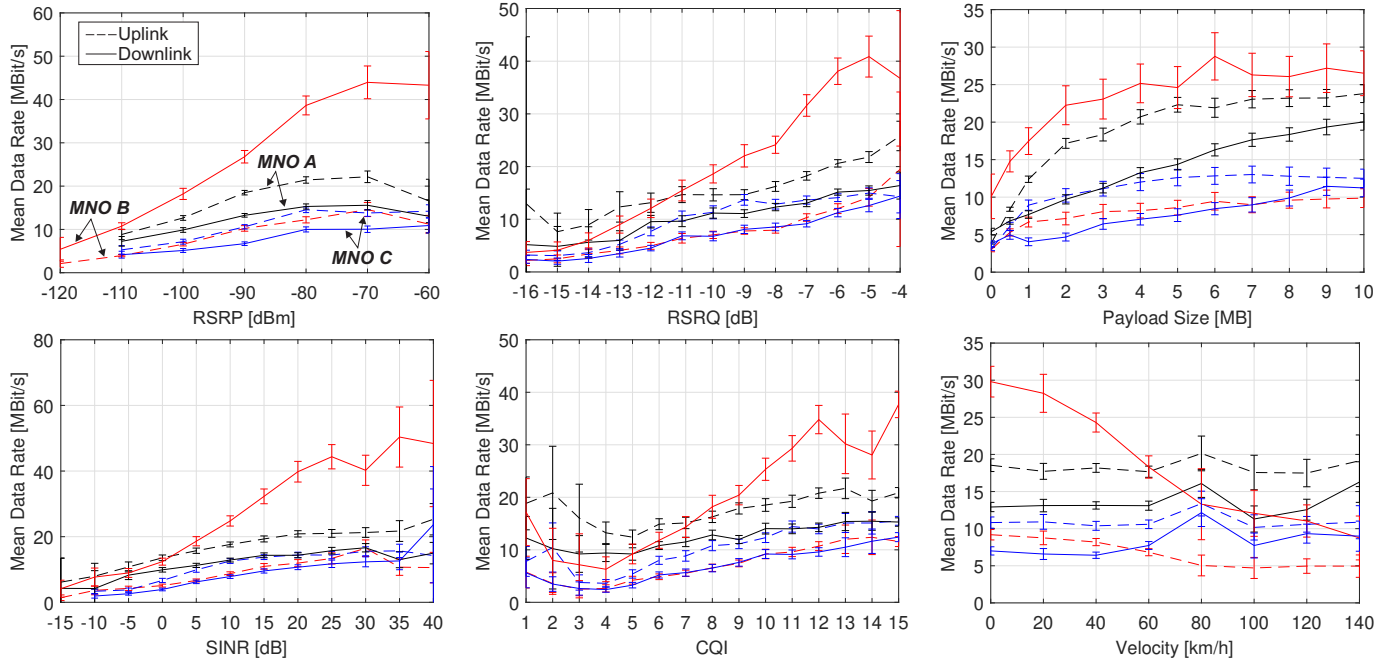


Fig. 5. Impact of the different indicators on the average resulting data rate for three network operators in uplink and downlink duration. The error bars illustrate the 0.95-confidence interval of the mean value.

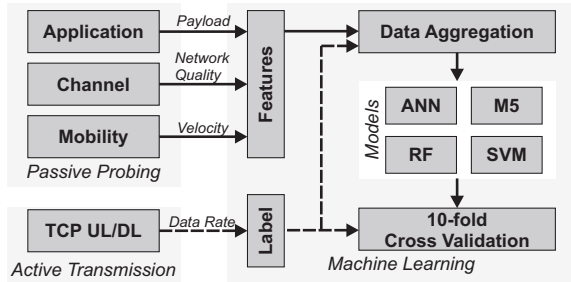


Fig. 6. Architecture model for client-based data rate prediction.

with two hidden layers (10 and 5 neurons) resulted in the best performance. Additional parameters (learning rate $\eta = 0.1$, momentum $\alpha = 0.001$) were tuned based on an evolutionary algorithm. The applied RF consists of with 100 random trees and the SVM is parameterized as a linear L2/L2 SVM with squared hinge loss. If not stated otherwise, all prediction results are obtained from 10-fold cross validation.

The applied feature vector consists of nine different features:

- As **application context features**, the payload size of the data packet
- **Channel context features** contain RSRP, RSRQ, SINR, CQI, Timing Advance (TA) and the carrier frequency f
- As **mobility context features**, the current velocity of the vehicle and the cell id

The *coefficient of determination* (R^2) is a statistical metric for analyzing the prediction performance of a regression model, which describes the amount of the response variable variation that can be explained by derived model. It is widely used for data rate prediction (e.g., [16], [17]) and computed as

$$R^2 = 1 - \frac{\sum_{i=1}^N (\hat{y}_i - y_i)^2}{\sum_{i=1}^N (\bar{y} - y_i)^2} \quad (1)$$

with \bar{y}_i being the mean measurement value, y_i being the current measurement and \hat{y}_i being the current prediction.

Before the actual prediction results are discussed, the correlation between different indicators and the resulting data rate is analyzed in Fig. 5. As it is also shown in Fig. 3, *MNO B* provides the highest data rates in the downlink direction.

The payload size has a significant impact on the achievable data rate for all MNOs and transmission directions. It is directly related to the slow start mechanism of TCP and the channel coherence time. However, the upper bound of the mean data rate is lower than the one of the network quality indicators. Although this fact shows that the channel quality is an important indicator for the achievable data rate, the consideration of a single network quality indicator does not allow to derive meaningful conclusions for the resulting end-to-end data rate. Therefore, it can be expected that the machine learning-based joint consideration of multiple indicators is able to better describe the contained cross-dependencies.

Apart from *MNO B*, the velocity does not have a severe impact on the data rate. As discussed earlier (see Sec. IV), the average RSRP for *MNO B* is lower than for the other MNOs. With higher speeds, the probability for cellular handovers is increased, which severely disturb active data transmissions.

A. Comparison of Different Data Aggregation Approaches

In order to determine the optimal properties of the training sets, different data aggregation methods are analyzed. There is a trade-off between using a higher amount of training data (a single global data set) and a deeper consideration of the infrastructure-specific configurations (many local data sets). Therefore, the following measurement subsets are evaluated for all of the considered prediction models:

- **MNO** uses the whole data per MNO (3 sets).
- **Scenario** divides the data for the different scenarios *campus*, *urban*, *suburban* and *highway* (12 sets).

TABLE II
COEFFICIENT OF DETERMINATION (R^2) FOR DIFFERENT MACHINE LEARNING MODELS AND DATA AGGREGATION LEVELS

	Data	MNO A				MNO B				MNO C			
		ANN	M5	RF	SVM	ANN	M5	RF	SVM	ANN	M5	RF	SVM
Uplink	MNO	0.685	0.754	0.8	0.71	0.46	0.658	0.707	0.594	0.69	0.779	0.82	0.728
	Scenario	0.729	0.779	0.806	0.683	0.49	0.572	0.633	0.555	0.489	0.64	0.686	0.572
	eNB	0.578	0.724	0.731	0.592	0.285	0.432	0.456	0.44	0.384	0.57	0.604	0.512
	Cell	0.532	0.687	0.715	0.58	0.275	0.412	0.444	0.397	0.355	0.505	0.505	0.424
Downlink	MNO	0.499	0.603	0.591	0.612	0.524	0.584	0.648	0.578	0.41	0.504	0.552	0.531
	Scenario	0.551	0.62	0.615	0.627	0.321	0.491	0.541	0.496	0.265	0.386	0.422	0.41
	eNB	0.34	0.551	0.552	0.58	0.263	0.317	0.357	0.362	0.151	0.323	0.334	0.361
	Cell	0.3	0.564	0.503	0.555	0.258	0.325	0.379	0.372	0.19	0.296	0.306	0.294

ANN: Artificial Neural Network, M5: M5 Regression Tree, RF: Random Forest, SVM: Support Vector Machine

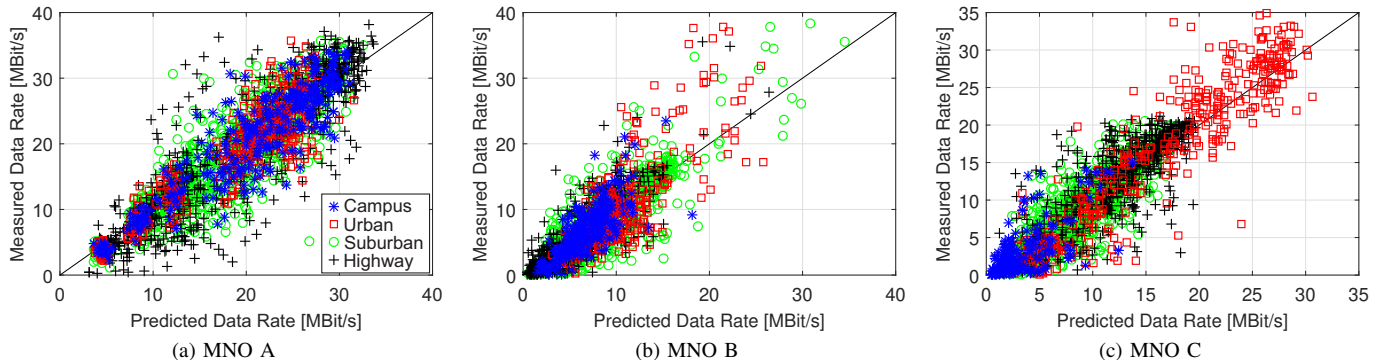


Fig. 7. Comparison of predictions and measurements for RF-based uplink data rate prediction for the considered MNOs in different scenarios. The black diagonal line illustrates perfect prediction. Data points in the upper left triangle represent underestimations of the data rate, elements in the lower right triangle overestimate the data rate.

- **eNB** groups the data based on the eNB id (105 sets).
- **Cell** performs cell id-specific data aggregation (220 sets).

Tab. II summarizes the results of the data rate prediction in uplink and downlink direction. For all considered MNOs, it can be seen that the R^2 is reduced when the grade of locality is increased. The highest value is achieved by the global data set, which contains all measurements per MNO. The prediction models benefit more from the additional data than from more context-specific data sets.

In most cases, the best prediction performance is achieved with the RF model. A possible explanation for this behavior is that in many situations, one of the considered network quality indicators has a dominant impact on the behavior of the data rate under defined conditions. The analysis in [3] points out that at the cell edge – which can be identified by the RSRP – the interference level, which is partly identifiable by the RSRQ, has a strong impact on the data rate. In contrast to that, the SINR is of higher importance within the cell center. These interval-wise scope regions match well with the general tree-like structure of RF and M5. Since Classification And Regression Tree (CART)-based models can be implemented in a very resource-efficient way as a sequence of *if/else* statements, this fact has positive implications on the resource efficiency for the online data rate prediction in the application phase of the models. In many cases, the M5 approach achieves the second highest R^2 value. This is remarkable, as the resulting trained model is significantly smaller than the RF. As an example for the full uplink data set of *MNO A*, the RF consists of 120533 leafs (numerical values) but the M5 has only 11 leafs (linear regression models). As a consequence, the M5 could be applied as a lightweight alternative to the RF for memory-constrained systems (e.g., microcontrollers).

It can be seen that the highest R^2 values are achieved for *MNO A* and *MNO C*. As the average RSRP of *MNO B* is low (see Tab. I), the probability for cellular handovers, which decrease the prediction accuracy, is higher than for the other MNOs, especially in the *campus* and *highway* scenarios.

The prediction works more precise in the uplink direction. As the traffic load in the uplink is usually much lower than in the downlink direction [1], the UE less likely encounters a loaded cell. Therefore, it can be concluded that the data rate is more impacted by the channel quality-related effects – which are covered to a high grade by the applied feature set – than by resource competition and scheduling-related aspects. While the consideration of the latter could likely improve the download prediction accuracy, this approach would require infrastructure side knowledge, which cannot be accessed using the proposed client-based approach. Based on the obtained insights, the following evaluations focus on RF-based uplink data rate prediction using the global MNO data sets.

A graphical representation of the resulting uplink data rate prediction performance of the trained RF models is shown in Fig. 7. It can be seen that the value range, error spread and the scenario-dependency is different for the considered MNOs. While *MNO A* shows a homogeneous behavior for all scenarios, both other MNOs have defined focus regions for the provided coverage. Fig. 8 shows the results of different combinations of training and test sets. The cross-MNO applicability of a trained model is evaluated in Fig. 8 (a). It can be seen that multi-MNO data rate prediction requires MNO-specific training of the machine learning models. This behavior can be explained by the usage of different network configurations with respect to resource scheduling, applied transmission power and distribution of the carrier frequencies.

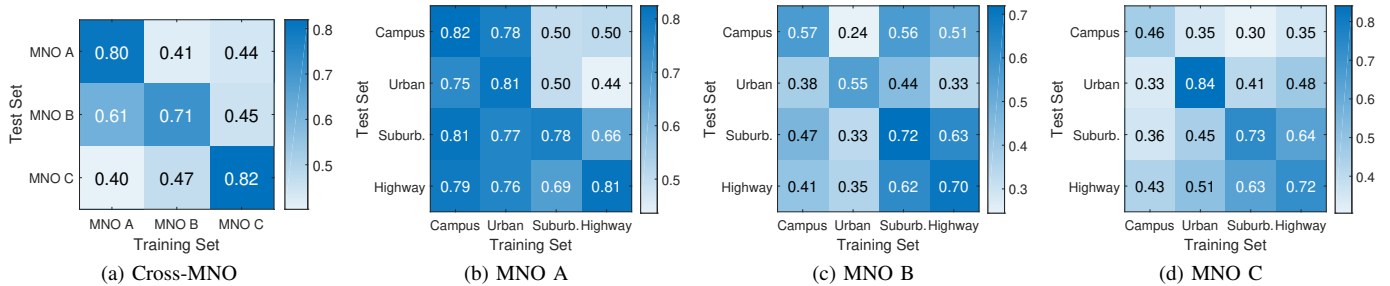


Fig. 8. R^2 results for RF-based uplink data rate prediction with different combinations of training and test sets. *Note:* For each element of the main diagonal, the results show the 10-fold cross validation on the training data in order to avoid interdependencies between training set and test set.

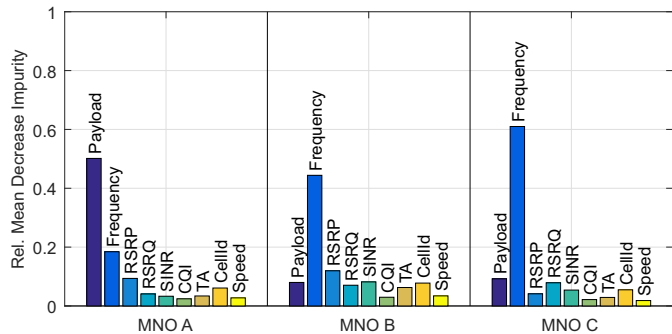


Fig. 9. Importance of individual features for RF-based uplink data rate prediction.

Furthermore, the applicability of cross-scenario training and testing is shown in Fig. 8 (b)-(d). For each MNO, a model is trained on the data of each individual scenario and tested against the data of the other scenarios. *MNO A* achieves very good generalization for the campus and urban scenarios but not for the suburban and highway scenarios. The results can be better understood by considering Fig. 7(a). The prediction model is very homogeneous for *MNO A* but the highest variance is shown by data points from the highway and suburban data set. For *MNO C*, the LTE coverage in the campus scenarios is only 76.25 %, which leads to a bad prediction performance for this scenario.

B. Feature Importance

Fig. 9 shows the relative average entropy-based Mean Decrease Impurity (MDI) [30] for the RF data rate prediction model for each MNO. Again, the considered MNOs show different behaviors. The features importance explains why the achieved overall prediction accuracy is significantly higher than the results achieved by related work, which only rely on passively measured network quality indicators ([16], [17], [14]). In addition to the carrier frequency, the payload size has a dominant impact on the prediction accuracy as it has different interdependencies to the network quality and the applied protocols. Larger packets likely correspond to longer transmission durations, which means that the dependency to the channel coherence time is increased as the vehicle is moving during the transmission process. Moreover, the TCP slow start is severely dependent on the packet size. For completeness, it should be remarked that the impact of other indicators (RTT, time of day) was analyzed in a preparatory step. As the integration of these indicators did not result in better prediction performance, they were not further evaluated.

We conclude that the added information is already immanently represented by the considered features, e.g. time of day has an impact on the cell load, which is correlated to the RSRQ.

C. Exploiting Multi-MNO Connectivity Maps for Data Rate Prediction

In the following, we analyze the suitability of using CMs for uplink data rate prediction in vehicular networks. In contrast to the previous measurement-based predictions approaches, the network quality is now solely looked up from the a priori information of the CMs based on the vehicle's location without performing dedicated radio quality measurements.

TABLE III
 R^2 AND MEAN ABSOLUTE ERROR (MAE) FOR RF-BASED PREDICTION WITH CONNECTIVITY MAPS AND DIFFERENT CELL SIZES IN THE UPLINK

Data	MNO A		MNO B		MNO C	
	R^2	MAE	R^2	MAE	R^2	MAE
MNO	0.8	2.92	0.707	2.3	0.82	2.27
CM ₅	0.797	3.02	0.71	2.23	0.851	2.16
CM ₁₀	0.861	2.42	0.716	2.22	0.852	2.15
CM ₂₅	0.856	2.56	0.719	2.21	0.852	2.11
CM ₅₀	0.857	2.43	0.719	2.22	0.851	2.12
CM ₁₀₀	0.844	2.54	0.714	2.22	0.846	2.14

CM_c: Connectivity map with cell size c [m], MNO: Total operator data set

Tab. III summarizes the R^2 and MAE values for the considered MNOs using different CM cell sizes. As a reference, the results for measurement-based MNO without CMs are shown. The choice of the cell size value represents the trade-off between using more data for the learning model and modeling a more specific representation of the environment. It can be assumed that the location information is influenced by Global Positioning System (GPS) positioning errors. Furthermore, the cell size defines the storage complexity of the CM model. It can be seen that the CM-based approach has different implications for the considered MNOs. While *MNO B* does not significantly benefit from using CMs, *MNO A* and *MNO C* achieve significant improvements of the prediction accuracy (for *MNO A*, the MAE is reduced by 17 % / 0.5 MBit/s). The prediction benefits from the cell-wise data aggregation performed by the CMs, which is able to compensate short-term influences such as multi-path fading. As a result, overfitting to a very specific radio channel situation is avoided and the resulting model achieves a better generalization.

For completeness, it should be noted that we investigated the combined usage of CM as well as measured features. Since this approach resulted in a similar performance as the pure CM-based version, it is not further evaluated.

VI. CONCLUSION

In this paper, we presented an empirical evaluation of multi-MNO communication for vehicular networks and analyzed the performance of multiple models for online data rate prediction. The analysis shows that even if one of the MNOs provides superior coverage and network quality, the overall performance can still be increased significantly by applying a multi-MNO approach. The achievable accuracy of data rate prediction is highly MNO-dependent. Therefore, data-driven multi-MNO approaches require different learning models for each considered MNO, which consequently increases the importance of the resource efficiency of the prediction models. In the majority of the considered cases, the RF model achieved the best prediction accuracy.

Although the channel properties have a significant impact on the achievable data rate, they need to be set into relation to the payload size in order to achieve precise predictions. This way, the machine learning process is able to consider hidden interdependencies between channel coherence time and network protocols. Connectivity maps can be utilized as a priori information to compensate short-term influences and can help to achieve a better generalization of the prediction schemes by avoiding overfitting. However, the achievable benefits of this approach and the optimal parametrization are also MNO-specific. In future work, we will leverage the prediction models for optimizing communication processes within context-predictive vehicular networks.

ACKNOWLEDGMENT

Part of the work on this paper has been supported by Deutsche Forschungsgemeinschaft (DFG) within the Collaborative Research Center SFB 876 "Providing Information by Resource-Constrained Analysis", project B4.

REFERENCES

- [1] N. Bui, M. Cesana, S. A. Hosseini, Q. Liao, I. Malanchini, and J. Widmer, "A survey of anticipatory mobile networking: Context-based classification, prediction methodologies, and optimization techniques," *IEEE Communications Surveys & Tutorials*, 2017.
- [2] B. Sliwa, T. Liebig, T. Vranken, M. Schreckenberger, and C. Wietfeld, "System-of-systems modeling, analysis and optimization of hybrid vehicular traffic," in *2019 Annual IEEE International Systems Conference (SysCon)*, Orlando, Florida, USA, Apr 2019.
- [3] B. Sliwa, T. Liebig, R. Falkenberg, J. Pillmann, and C. Wietfeld, "Efficient machine-type communication using multi-metric context-awareness for cars used as mobile sensors in upcoming 5G networks," in *2018 IEEE 87th Vehicular Technology Conference (VTC-Spring)*, Porto, Portugal, Jun 2018, Best Student Paper Award.
- [4] B. Sliwa, D. Behnke, C. Ide, and C. Wietfeld, "B.A.T.Mobile: Leveraging mobility control knowledge for efficient routing in mobile robotic networks," in *IEEE GLOBECOM 2016 Workshop on Wireless Networking, Control and Positioning of Unmanned Autonomous Vehicles (Wi-UAV)*, Washington D.C., USA, Dec 2016.
- [5] B. Sliwa, T. Liebig, R. Falkenberg, J. Pillmann, and C. Wietfeld, "Machine learning based context-predictive car-to-cloud communication using multi-layer connectivity maps for upcoming 5G networks," in *2018 IEEE 88th Vehicular Technology Conference (VTC-Fall)*, Chicago, USA, Aug 2018.
- [6] B. Sliwa, R. Falkenberg, T. Liebig, N. Piatkowski, and C. Wietfeld, "Boosting vehicle-to-cloud communication by machine learning-enabled context prediction," *IEEE Transactions on Intelligent Transportation Systems*, 2019, Accepted for publication.
- [7] B. Sliwa and C. Wietfeld, "Towards data-driven simulation of end-to-end network performance indicators," in *2019 IEEE 90th Vehicular Technology Conference (VTC-Fall)*, Honolulu, Hawaii, USA, Sep 2019.
- [8] H. Ye, L. Liang, G. Y. Li, J. Kim, L. Lu, and M. Wu, "Machine learning for vehicular networks: Recent advances and application examples," *IEEE Vehicular Technology Magazine*, vol. 13, no. 2, pp. 94–101, June 2018.
- [9] C. Jiang, H. Zhang, Y. Ren, Z. Han, K. C. Chen, and L. Hanzo, "Machine learning paradigms for next-generation wireless networks," *IEEE Wireless Communications*, vol. 24, no. 2, pp. 98–105, April 2017.
- [10] E. A. Walelgne, J. Manner, V. Bajpai, and J. Ott, "Analyzing throughput and stability in cellular networks," in *NOMS 2018 - 2018 IEEE/IFIP Network Operations and Management Symposium*, April 2018, pp. 1–9.
- [11] M. Akselrod, N. Becker, M. Fidler, and R. Luebben, "4G LTE on the road - what impacts download speeds most?" in *2017 IEEE 86th Vehicular Technology Conference (VTC-Fall)*, Sep. 2017, pp. 1–6.
- [12] E. R. Cavalcanti, J. A. R. de Souza, M. A. Spohn, R. C. d. M. Gomes, and A. F. B. F. d. Costa, "VANETs' research over the past decade: Overview, credibility, and trends," *SIGCOMM Comput. Commun. Rev.*, vol. 48, no. 2, pp. 31–39, May 2018.
- [13] S. S. Chaudhari and R. C. Biradar, "Survey of bandwidth estimation techniques in communication networks," *Wireless Personal Communications*, vol. 83, no. 2, pp. 1425–1476, Jul 2015.
- [14] J. Riihijarvi and P. Mahonen, "Machine learning for performance prediction in mobile cellular networks," *IEEE Computational Intelligence Magazine*, vol. 13, no. 1, pp. 51–60, Feb 2018.
- [15] J. Caaney, B. Gill, S. Johnston, J. Robinson, and S. Westwood, "Modelling download throughput of LTE networks," in *39th Annual IEEE Conference on Local Computer Networks Workshops*, Sep. 2014, pp. 623–628.
- [16] F. Jomrich, A. Herzberger, T. Meuser, B. Richerzhagen, R. Steinmetz, and C. Wille, "Cellular bandwidth prediction for highly automated driving - Evaluation of machine learning approaches based on real-world data," in *Proceedings of the 4th International Conference on Vehicle Technology and Intelligent Transport Systems 2018*, no. 4, SCITEPRESS, Mar 2018, pp. 121–131.
- [17] A. Samba, Y. Busnel, A. Blanc, P. Dooze, and G. Simon, "Instantaneous throughput prediction in cellular networks: Which information is needed?" in *2017 IFIP/IEEE Symposium on Integrated Network and Service Management (IM)*, May 2017, pp. 624–627.
- [18] K. Kousias, C. Midoglu, O. Alay, A. Lutu, A. Argyriou, and M. Riegler, "The same, only different: Contrasting mobile operator behavior from crowdsourced dataset," in *2017 IEEE 28th Annual International Symposium on Personal, Indoor, and Mobile Radio Communications (PIMRC)*, Oct 2017, pp. 1–6.
- [19] G. Nikolov, M. Kuhn, and B. Wenning, "UE-based estimation of available uplink data rates in cellular networks," in *2018 14th International Conference on Wireless and Mobile Computing, Networking and Communications (WiMob)*, Oct 2018, pp. 169–174.
- [20] M. Kasparick, R. L. G. Cavalcante, S. Valentin, S. Stańczak, and M. Yukawa, "Kernel-based adaptive online reconstruction of coverage maps with side information," *IEEE Transactions on Vehicular Technology*, vol. 65, no. 7, pp. 5461–5473, July 2016.
- [21] K. Apajalahti, E. A. Walelgne, J. Manner, and E. Hyvönen, "Correlation-based feature mapping of crowdsourced LTE data," in *2018 IEEE 29th Annual International Symposium on Personal, Indoor and Mobile Radio Communications (PIMRC)*, Sep. 2018, pp. 1–7.
- [22] B. Sliwa, "Raw experimental cellular network quality data," Februar 2019. [Online]. Available: <http://doi.org/10.5281/zenodo.2553832>
- [23] M. Hall, E. Frank, G. Holmes, B. Pfahringer, P. Reutemann, and I. H. Witten, "The WEKA data mining software: An update," *SIGKDD Explorations*, vol. 11, no. 1, pp. 10–18, 2009.
- [24] C.-C. Chang and C.-J. Lin, "LIBSVM: A library for support vector machines," *ACM Trans. Intell. Syst. Technol.*, vol. 2, no. 3, pp. 27:1–27:27, May 2011.
- [25] R. Falkenberg, B. Sliwa, N. Piatkowski, and C. Wietfeld, "Machine learning based uplink transmission power prediction for LTE and upcoming 5G networks using passive downlink indicators," in *2018 IEEE 88th Vehicular Technology Conference (VTC-Fall)*, Chicago, USA, Aug 2018.
- [26] Y. LeCun, Y. Bengio, and G. Hinton, "Deep learning," *Nature*, vol. 521, no. 7553, pp. 436–444, 5 2015.
- [27] J. R. Quinlan, "Learning with continuous classes." World Scientific, 1992, pp. 343–348.
- [28] L. Breiman, "Random forests," *Mach. Learn.*, vol. 45, no. 1, pp. 5–32, Oct. 2001.
- [29] C. Cortes and V. Vapnik, "Support-vector networks," *Mach. Learn.*, vol. 20, no. 3, pp. 273–297, Sep. 1995.
- [30] G. Louppe, L. Wehenkel, A. Suter, and P. Geurts, "Understanding variable importances in forests of randomized trees," in *Proceedings of the 26th International Conference on Neural Information Processing Systems - Volume 1*, ser. NIPS'13. USA: Curran Associates Inc., 2013, pp. 431–439.